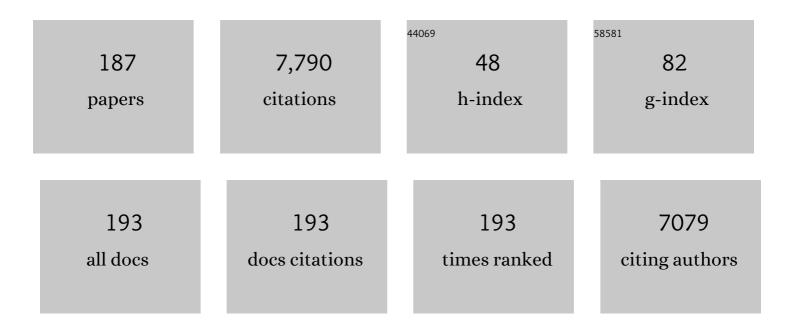
List of Publications by Year in descending order

Source: https://exaly.com/author-pdf/336084/publications.pdf Version: 2024-02-01



#	Article	IF	CITATIONS
1	Impact of coronary revascularization and transmural extent of scar on regional left ventricular remodelling. European Heart Journal, 2008, 29, 1608-1617.	2.2	427
2	Shear properties of passive ventricular myocardium. American Journal of Physiology - Heart and Circulatory Physiology, 2002, 283, H2650-H2659.	3.2	288
3	UK Biobank's cardiovascular magnetic resonance protocol. Journal of Cardiovascular Magnetic Resonance, 2016, 18, 8.	3.3	254
4	The Cardiac Atlas Project—an imaging database for computational modeling and statistical atlases of the heart. Bioinformatics, 2011, 27, 2288-2295.	4.1	232
5	AI in Medical Imaging Informatics: Current Challenges and Future Directions. IEEE Journal of Biomedical and Health Informatics, 2020, 24, 1837-1857.	6.3	215
6	Tracking and finite element analysis of stripe deformation in magnetic resonance tagging. IEEE Transactions on Medical Imaging, 1995, 14, 413-421.	8.9	205
7	Left Ventricular Mass and Volume: Fast Calculation with Guide-Point Modeling on MR Images. Radiology, 2000, 216, 597-602.	7.3	202
8	lmaging in population science: cardiovascular magnetic resonance in 100,000 participants of UK Biobank - rationale, challenges and approaches. Journal of Cardiovascular Magnetic Resonance, 2013, 15, 46.	3.3	188
9	Multiphysics and multiscale modelling, data–model fusion and integration of organ physiology in the clinic: ventricular cardiac mechanics. Interface Focus, 2016, 6, 20150083.	3.0	165
10	Machine learning in cardiovascular magnetic resonance: basic concepts and applications. Journal of Cardiovascular Magnetic Resonance, 2019, 21, 61.	3.3	157
11	Modelling passive diastolic mechanics with quantitative MRI of cardiac structure and function. Medical Image Analysis, 2009, 13, 773-784.	11.6	155
12	Extended confocal microscopy of myocardial laminae and collagen network. Journal of Microscopy, 1998, 192, 139-150.	1.8	150
13	Regeneration of the Heart in Diabetes by Selective Copper Chelation. Diabetes, 2004, 53, 2501-2508.	0.6	143
14	A collaborative resource to build consensus for automated left ventricular segmentation of cardiac MR images. Medical Image Analysis, 2014, 18, 50-62.	11.6	143
15	Quantification of LV function and mass by cardiovascular magnetic resonance: multi-center variability and consensus contours. Journal of Cardiovascular Magnetic Resonance, 2015, 17, 63.	3.3	135
16	Impaired subendocardial contractile myofiber function in asymptomatic aged humans, as detected using MRI. American Journal of Physiology - Heart and Circulatory Physiology, 2006, 291, H1573-H1579.	3.2	134
17	Deformable models with parameter functions for cardiac motion analysis from tagged MRI data. IEEE Transactions on Medical Imaging, 1996, 15, 278-289.	8.9	131
18	Assessments of Right Ventricular Volume and Function Using Three-Dimensional Echocardiography in Older Children and Adults With Congenital Heart Disease: Comparison With Cardiac Magnetic Resonance Imaging. Journal of the American Society of Echocardiography, 2009, 22, 1279-1288.	2.8	127

#	Article	IF	CITATIONS
19	Three-dimensional assessment of left ventricular systolic strain in patients with type 2 diabetes mellitus, diastolic dysfunction, and normal ejection fraction. American Journal of Cardiology, 2004, 94, 1391-1395.	1.6	117
20	Computational cardiac atlases: from patient to population and back. Experimental Physiology, 2009, 94, 578-596.	2.0	115
21	MRI phase contrast velocity and flow errors in turbulent stenotic jets. Journal of Magnetic Resonance Imaging, 2008, 28, 210-218.	3.4	112
22	Applications and Comparisons of Four Time Series Models in Epidemiological Surveillance Data. PLoS ONE, 2014, 9, e88075.	2.5	109
23	Regional heterogeneity of function in nonischemic dilated cardiomyopathy. Cardiovascular Research, 2001, 49, 308-318.	3.8	95
24	Evaluation of left ventricular torsion by cardiovascular magnetic resonance. Journal of Cardiovascular Magnetic Resonance, 2012, 14, 49.	3.3	94
25	Comparative Study of Four Time Series Methods in Forecasting Typhoid Fever Incidence in China. PLoS ONE, 2013, 8, e63116.	2.5	92
26	Age-Related Changes in Myocardial Relaxation Using Three-Dimensional Tagged Magnetic Resonance Imaging. Journal of Cardiovascular Magnetic Resonance, 2003, 5, 421-430.	3.3	88
27	A Triaxial-Measurement Shear-Test Device for Soft Biological Tissues. Journal of Biomechanical Engineering, 2000, 122, 471-478.	1.3	87
28	Aging alters patterns of regional nonuniformity in LV strain relaxation: a 3-D MR tissue tagging study. American Journal of Physiology - Heart and Circulatory Physiology, 2003, 285, H621-H630.	3.2	87
29	Comparison of magnetic resonance feature tracking for systolic and diastolic strain and strain rate calculation with spatial modulation of magnetization imaging analysis. Journal of Magnetic Resonance Imaging, 2015, 41, 1000-1012.	3.4	87
30	Semi-automatic tracking of myocardial motion in MR tagged images. IEEE Transactions on Medical Imaging, 1995, 14, 422-433.	8.9	82
31	Model tags: direct three-dimensional tracking of heart wall motion from tagged magnetic resonance images. Medical Image Analysis, 1999, 3, 361-372.	11.6	77
32	3-Dimensional configuration of perimysial collagen fibres in rat cardiac muscle at resting and extended sarcomere lengths. Journal of Physiology, 1999, 517, 831-837.	2.9	76
33	t-tubule disease: Relationship between t-tubule organization and regional contractile performance in human dilated cardiomyopathy. Journal of Molecular and Cellular Cardiology, 2015, 84, 170-178.	1.9	76
34	Left ventricular shape variation in asymptomatic populations: the multi-ethnic study of atherosclerosis. Journal of Cardiovascular Magnetic Resonance, 2014, 16, 56.	3.3	75
35	Right ventricular regional function using MR tagging: Normals versus chronic pulmonary hypertension. Magnetic Resonance in Medicine, 1998, 39, 116-123.	3.0	71
36	A copper(II)-selective chelator ameliorates left-ventricular hypertrophy in type 2 diabetic patients: a randomised placebo-controlled study. Diabetologia, 2009, 52, 715-722.	6.3	70

ALISTAIR A YOUNG

#	Article	IF	CITATIONS
37	Atlas-Based Quantification of Cardiac Remodeling Due to Myocardial Infarction. PLoS ONE, 2014, 9, e110243.	2.5	65
38	Nonhomogeneous analysis of epicardial strain distributions during acute myocardial ischemia in the dog. Journal of Biomechanics, 1993, 26, 19-35.	2.1	64
39	Myocardial material parameter estimation. Biomechanics and Modeling in Mechanobiology, 2008, 7, 161-173.	2.8	61
40	Statistical Shape Modeling of the Left Ventricle: Myocardial Infarct Classification Challenge. IEEE Journal of Biomedical and Health Informatics, 2018, 22, 503-515.	6.3	61
41	4DFlowNet: Super-Resolution 4D Flow MRI Using Deep Learning and Computational Fluid Dynamics. Frontiers in Physics, 2020, 8, .	2.1	61
42	Phase contrast ultrashort TE: A more reliable technique for measurement of highâ€velocity turbulent stenotic jets. Magnetic Resonance in Medicine, 2009, 62, 626-636.	3.0	59
43	Hemodynamics in Idealized Stented Coronary Arteries: Important Stent Design Considerations. Annals of Biomedical Engineering, 2016, 44, 315-329.	2.5	59
44	Method and Apparatus for Soft Tissue Material Parameter Estimation Using Tissue Tagged Magnetic Resonance Imaging. Journal of Biomechanical Engineering, 2005, 127, 148-157.	1.3	58
45	Effect of Spironolactone on Left Ventricular Systolic and Diastolic Function in Patients With Early Stage Chronic Kidney Disease. American Journal of Cardiology, 2010, 106, 1505-1511.	1.6	55
46	Generalized spatiotemporal myocardial strain analysis for DENSE and SPAMM imaging. Magnetic Resonance in Medicine, 2012, 67, 1590-1599.	3.0	55
47	In-line Automated Tracking for Ventricular Function With Magnetic Resonance Imaging. JACC: Cardiovascular Imaging, 2010, 3, 860-866.	5.3	53
48	Multi-parameter in vivo cardiac magnetic resonance imaging demonstrates normal perfusion reserve despite severely attenuated β-adrenergic functional response in neuronal nitric oxide synthase knockout mice. European Heart Journal, 2007, 28, 2792-2798.	2.2	51
49	Left ventricular hypertrophy and renin-angiotensin system blockade. Current Hypertension Reports, 2009, 11, 167-72.	3.5	50
50	Epicardial surface estimation from coronary angiograms. Computer Vision, Graphics, and Image Processing, 1989, 47, 111-127.	1.0	48
51	Automatic initialization and quality control of large-scale cardiac MRI segmentations. Medical Image Analysis, 2018, 43, 129-141.	11.6	48
52	Estimation of epicardial strain using the motions of coronary bifurcations in biplane cineangiography. IEEE Transactions on Biomedical Engineering, 1992, 39, 526-531.	4.2	47
53	Right ventricular shape and function: cardiovascular magnetic resonance reference morphology and biventricular risk factor morphometrics in UK Biobank. Journal of Cardiovascular Magnetic Resonance, 2019, 21, 41.	3.3	47
54	Left Ventricular Mass and Volume With Telmisartan, Ramipril, or Combination in Patients With Previous Atherosclerotic Events or With Diabetes Mellitus (from the ONgoing Telmisartan Alone and) Tj ETQq 2009, 104, 1484-1489.	0 0 0 1gBT /0	Overlock 10 Tf

#	Article	IF	CITATIONS
55	Aortic valve stenotic area calculation from phase contrast cardiovascular magnetic resonance: the importance of short echo time. Journal of Cardiovascular Magnetic Resonance, 2009, 11, 49.	3.3	46
56	Fully-automated left ventricular mass and volume MRI analysis in the UK Biobank population cohort: evaluation of initial results. International Journal of Cardiovascular Imaging, 2018, 34, 281-291.	1.5	46
57	Left ventricular shape predicts different types of cardiovascular events in the general population. Heart, 2017, 103, 499-507.	2.9	45
58	Impact of bifurcation angle and other anatomical characteristics on blood flow – A computational study of non-stented and stented coronary arteries. Journal of Biomechanics, 2016, 49, 1570-1582.	2.1	44
59	Changes in Cardiac Morphology and Function in Individuals With Diabetes Mellitus. Circulation: Cardiovascular Imaging, 2019, 12, e009476.	2.6	43
60	Independent Left Ventricular Morphometric Atlases Show Consistent Relationships with Cardiovascular Risk Factors: A UK Biobank Study. Scientific Reports, 2019, 9, 1130.	3.3	43
61	A computational atlas of normal coronary artery anatomy. EuroIntervention, 2016, 12, 845-854.	3.2	43
62	Reperfused Myocardial Infarction in Mice: 3D Mapping of Late Gadolinium Enhancement and Strain. Journal of Cardiovascular Magnetic Resonance, 2006, 8, 685-692.	3.3	42
63	The effect of synthetic patch repair of coarctation on regional deformation of the aortic wall. Journal of Thoracic and Cardiovascular Surgery, 2000, 120, 1053-1063.	0.8	39
64	Big Heart Data: Advancing Health Informatics Through Data Sharing in Cardiovascular Imaging. IEEE Journal of Biomedical and Health Informatics, 2015, 19, 1283-1290.	6.3	39
65	Extraction and Quantification of Left Ventricular Deformation Modes. IEEE Transactions on Biomedical Engineering, 2004, 51, 1923-1931.	4.2	37
66	A randomized trial of the aldosterone-receptor antagonist eplerenone in asymptomatic moderate-severe aortic stenosis. American Heart Journal, 2008, 156, 348-355.	2.7	37
67	Treatment with a copper-selective chelator causes substantive improvement in cardiac function of diabetic rats with left-ventricular impairment. Cardiovascular Diabetology, 2013, 12, 28.	6.8	36
68	Marked Regional Left Ventricular Heterogeneity in Hypertensive Left Ventricular Hypertrophy Patients. Hypertension, 2008, 52, 279-286.	2.7	34
69	Left Ventricular Diastolic Myocardial Stiffness and End-Diastolic Myofibre Stress in Human Heart Failure Using Personalised Biomechanical Analysis. Journal of Cardiovascular Translational Research, 2018, 11, 346-356.	2.4	34
70	Integrated MRI assessment of regional function and perfusion in canine myocardial infarction. Magnetic Resonance in Medicine, 1998, 40, 311-326.	3.0	31
71	Automated Detection of Left Ventricle in 4D MR Images: Experience from a Large Study. Lecture Notes in Computer Science, 2006, 9, 728-735.	1.3	31
72	Relationship between QRS duration and left ventricular mass and volume in patients at high cardiovascular risk. Heart, 2011, 97, 1766-1770.	2.9	31

#	Article	IF	CITATIONS
73	Atlas-based analysis of cardiac shape and function: correction of regional shape bias due to imaging protocol for population studies. Journal of Cardiovascular Magnetic Resonance, 2013, 15, 80.	3.3	30
74	Fully Automated Myocardial Strain Estimation from Cardiovascular MRI–tagged Images Using a Deep Learning Framework in the UK Biobank. Radiology: Cardiothoracic Imaging, 2020, 2, e190032.	2.5	29
75	Pilot Study to Assess the Influence of β-Blockade on Mitral Regurgitant Volume and Left Ventricular Work in Degenerative Mitral Valve Disease. Circulation, 2008, 118, 1041-1046.	1.6	26
76	Left Ventricular Segmentation Challenge from Cardiac MRI: A Collation Study. Lecture Notes in Computer Science, 2012, , 88-97.	1.3	26
77	Parameter distribution models for estimation of population based left ventricular deformation using sparse fiducial markers. IEEE Transactions on Medical Imaging, 2005, 24, 381-388.	8.9	23
78	Estimation of Cardiac Hyperelastic Material Properties from MRI Tissue Tagging and Diffusion Tensor Imaging. Lecture Notes in Computer Science, 2006, 9, 628-635.	1.3	23
79	Cardiac image modelling: Breadth and depth in heart disease. Medical Image Analysis, 2016, 33, 38-43.	11.6	23
80	A Study of Coronary Bifurcation Shape in a Normal Population. Journal of Cardiovascular Translational Research, 2017, 10, 82-90.	2.4	22
81	Temporal Evolution of Left Ventricular Strain Late After Repair of Coarctation of the Aorta Using 3D MR Tissue Tagging. Journal of Cardiovascular Magnetic Resonance, 2002, 4, 233-243.	3.3	20
82	Information maximizing component analysis of left ventricular remodeling due to myocardial infarction. Journal of Translational Medicine, 2015, 13, 343.	4.4	20
83	Real-time aortic pulse wave velocity measurement during exercise stress testing. Journal of Cardiovascular Magnetic Resonance, 2015, 17, 86.	3.3	20
84	Atlas-based ventricular shape analysis for understanding congenital heart disease. Progress in Pediatric Cardiology, 2016, 43, 61-69.	0.4	20
85	Artificial Intelligence in Cardiac Imaging With Statistical Atlases of Cardiac Anatomy. Frontiers in Cardiovascular Medicine, 2020, 7, 102.	2.4	20
86	Changes in Mitral Annular Geometry and Dynamics With β-Blockade in Patients With Degenerative Mitral Valve Disease. Circulation: Cardiovascular Imaging, 2010, 3, 687-693.	2.6	19
87	Atlas-Based Computational Analysis of Heart Shape and Function in Congenital Heart Disease. Journal of Cardiovascular Translational Research, 2018, 11, 123-132.	2.4	19
88	Cardiac Anchoring in MRI through Context Modeling. Lecture Notes in Computer Science, 2010, 13, 383-390.	1.3	19
89	Feasibility of single breath-hold left ventricular function with 3 Tesla TSENSE acquisition and 3D modeling analysis. Journal of Cardiovascular Magnetic Resonance, 2008, 10, 24.	3.3	18
90	An Open Benchmark Challenge for Motion Correction of Myocardial Perfusion MRI. IEEE Journal of Biomedical and Health Informatics, 2017, 21, 1315-1326.	6.3	18

#	Article	IF	CITATIONS
91	Image-Based Investigation of Human in Vivo Myofibre Strain. IEEE Transactions on Medical Imaging, 2016, 35, 2486-2496.	8.9	17
92	Estimation of transversely isotropic material properties from magnetic resonance elastography using the optimised virtual fields method. International Journal for Numerical Methods in Biomedical Engineering, 2018, 34, e2979.	2.1	17
93	Midwall Shortening After Coarctation Repair: The Effect of Through-plane Motion on Single-plane Indices of Left Ventricular Function. Journal of the American Society of Echocardiography, 2005, 18, 1131-1136.	2.8	15
94	Development of a method for the measurement of primary cilia length in 3D. Cilia, 2012, 1, 11.	1.8	15
95	Image Feature Determinants of Global and Segmental Circumferential Ventricular Strain From Cine CMR. JACC: Cardiovascular Imaging, 2015, 8, 1465-1466.	5.3	15
96	Morphologically normalized left ventricular motion indicators from MRI feature tracking characterize myocardial infarction. Scientific Reports, 2017, 7, 12259.	3.3	15
97	Right-left ventricular shape variations in tetralogy of Fallot: associations with pulmonary regurgitation. Journal of Cardiovascular Magnetic Resonance, 2021, 23, 105.	3.3	15
98	Challenges of Cardiac Image Analysis in Large-Scale Population-Based Studies. Current Cardiology Reports, 2015, 17, 563.	2.9	14
99	Increased cardiac work provides a link between systemic hypertension and heart failure. Physiological Reports, 2017, 5, e13104.	1.7	14
100	Four-dimensional flow cardiovascular magnetic resonance in tetralogy of Fallot: a systematic review. Journal of Cardiovascular Magnetic Resonance, 2021, 23, 59.	3.3	14
101	The visualization and measurement of left ventricular deformation using finite element models. Journal of Visual Languages and Computing, 2003, 14, 299-326.	1.8	13
102	Fast left ventricular mass and volume assessment in mice with threeâ€dimensional guideâ€point modeling. Journal of Magnetic Resonance Imaging, 2009, 30, 514-520.	3.4	13
103	Noninvasive quantification of cerebrovascular pressure changes using 4D Flow MRI. Magnetic Resonance in Medicine, 2021, 86, 3096-3110.	3.0	13
104	A three-dimensional atlas of child's cardiac anatomy and the unique morphological alterations associated with obesity. European Heart Journal Cardiovascular Imaging, 2022, 23, 1645-1653.	1.2	13
105	Image-driven constitutive modeling of myocardial fibrosis. International Journal for Computational Methods in Engineering Science and Mechanics, 2016, 17, 211-221.	2.1	12
106	Long-term cardiovascular outcome following fetal anaemia and intrauterine transfusion: a cohort study. Archives of Disease in Childhood, 2017, 102, 40-45.	1.9	12
107	Orthogonal decomposition of left ventricular remodeling in myocardial infarction. GigaScience, 2017, 6, 1-15.	6.4	12
108	Microstructurally Motivated Constitutive Modeling of Heart Failure Mechanics. Biophysical Journal, 2019, 117, 2273-2286.	0.5	12

#	Article	IF	CITATIONS
109	An Implementation of Patient-Specific Biventricular Mechanics Simulations With a Deep Learning and Computational Pipeline. Frontiers in Physiology, 2021, 12, 716597.	2.8	12
110	The cardiac MRI substudy to ongoing telmisartan alone and in combination with ramipril global endpoint trial/telmisartan randomized assessment study in ACE-intolerant subjects with cardiovascular disease: analysis protocol and baseline characteristics. Clinical Research in Cardiology, 2009, 98, 421-433.	3.3	11
111	Construction of a Coronary Artery Atlas from CT Angiography. Lecture Notes in Computer Science, 2014, 17, 513-520.	1.3	11
112	Rapid D-Affine Biventricular Cardiac Function with Polar Prediction. Lecture Notes in Computer Science, 2014, 17, 546-553.	1.3	11
113	Myocardial Contractility and Regional Work throughout the Cardiac Cycle Using FEM and MRI. Lecture Notes in Computer Science, 2012, , 149-159.	1.3	11
114	Large Scale Left Ventricular Shape Atlas Using Automated Model Fitting to Contours. Lecture Notes in Computer Science, 2013, , 433-441.	1.3	11
115	Model tags: Direct 3D tracking of heart wall motion from tagged MR images. Lecture Notes in Computer Science, 1998, , 92-101.	1.3	10
116	GPU Accelerated Non-rigid Registration for the Evaluation of Cardiac Function. Lecture Notes in Computer Science, 2008, 11, 880-887.	1.3	10
117	Cardiac Image Modeling Tool for Quantitative Analysis of Global and Regional Cardiac Wall Motion. Investigative Radiology, 2009, 44, 271-278.	6.2	10
118	Accelerating global left-ventricular function assessment in mice using reduced slice acquisition and three-dimensional guide-point modelling. Journal of Cardiovascular Magnetic Resonance, 2011, 13, 49.	3.3	10
119	Cardiovascular Magnetic Resonance: Deeper Insights Through Bioengineering. Annual Review of Biomedical Engineering, 2013, 15, 433-461.	12.3	10
120	Systematic Comparison of Left Ventricular Geometry Between 3D-Echocardiography and Cardiac Magnetic Resonance Imaging. Frontiers in Cardiovascular Medicine, 2021, 8, 728205.	2.4	10
121	Three-Dimensional Volumetric Assessment of Diastolic Function by Cardiac Magnetic Resonance Imaging: The Multi-Ethnic Study of Atherosclerosis (MESA). Arquivos Brasileiros De Cardiologia, 2017, 108, 552-563.	0.8	10
122	An interactive tool for rapid biventricular analysis of congenital heart disease. Clinical Physiology and Functional Imaging, 2017, 37, 413-420.	1.2	9
123	Editorial: Current and Future Role of Artificial Intelligence in Cardiac Imaging. Frontiers in Cardiovascular Medicine, 2020, 7, 137.	2.4	9
124	Ex vivo cardiovascularÂmagnetic resonance diffusion weighted imaging in congenital heart disease, an insight into the microstructures of tetralogy of Fallot, biventricular and univentricular systemic right ventricle. Journal of Cardiovascular Magnetic Resonance, 2020, 22, 69.	3.3	9
125	Cardiac Active Contraction Parameters Estimated from Magnetic Resonance Imaging. Lecture Notes in Computer Science, 2010, , 194-203.	1.3	9
126	Changes in In Vivo Myocardial Tissue Properties Due to Heart Failure. Lecture Notes in Computer Science, 2013, , 216-223.	1.3	9

#	Article	IF	CITATIONS
127	WSSNet: Aortic Wall Shear Stress Estimation Using Deep Learning on 4D Flow MRI. Frontiers in Cardiovascular Medicine, 2021, 8, 769927.	2.4	9
128	Myocardial mesostructure and mesofunction. American Journal of Physiology - Heart and Circulatory Physiology, 2022, 323, H257-H275.	3.2	9
129	Strain softening behaviour in nonviable rat right-ventricular trabeculae, in the presence and the absence of butanedione monoxime. Experimental Physiology, 2004, 89, 593-604.	2.0	8
130	Estimation of myocardial strain from non-rigid registration and highly accelerated cine CMR. International Journal of Cardiovascular Imaging, 2017, 33, 101-107.	1.5	8
131	Deep Learning Analysis of Cardiac MRI in Legacy Datasets: Multi-Ethnic Study of Atherosclerosis. Frontiers in Cardiovascular Medicine, 2021, 8, 807728.	2.4	8
132	Right Ventricular Flow Vorticity Relationships With Biventricular Shape in Adult Tetralogy of Fallot. Frontiers in Cardiovascular Medicine, 2021, 8, 806107.	2.4	8
133	Passive Ventricular Mechanics Modelling Using MRI of Structure and Function. Lecture Notes in Computer Science, 2008, 11, 814-821.	1.3	7
134	Mapping system for coregistration of cardiac mri and ex vivo tissue sampling. Journal of Magnetic Resonance Imaging, 2011, 34, 1065-1071.	3.4	7
135	Ventricular Torsion. JACC: Cardiovascular Imaging, 2012, 5, 282-284.	5.3	7
136	Comparison of effects of losartan and metoprolol on left ventricular and aortic function at rest and during exercise in chronic aortic regurgitation. International Journal of Cardiovascular Imaging, 2018, 34, 615-624.	1.5	7
137	Efficient estimation of loadâ€free left ventricular geometry and passive myocardial properties using principal component analysis. International Journal for Numerical Methods in Biomedical Engineering, 2020, 36, e3313.	2.1	7
138	An Atlas for Cardiac MRI Regional Wall Motion and Infarct Scoring. Lecture Notes in Computer Science, 2013, , 188-197.	1.3	7
139	Assessment of Cardiac Performance with Magnetic Resonance Imaging. Current Cardiology Reviews, 2006, 2, 271-282.	1.5	6
140	Low vitamin D levels are related to left ventricular concentric remodelling in men of different ethnic groups with varying cardiovascular risk. International Journal of Cardiology, 2012, 158, 444-447.	1.7	6
141	Atlas-based anatomical modeling and analysis of heart disease. Drug Discovery Today: Disease Models, 2014, 14, 33-39.	1.2	6
142	The Cardiac Atlas Project: Preliminary Description of Heart Shape in Patients with Myocardial Infarction. Lecture Notes in Computer Science, 2010, , 46-53.	1.3	6
143	Finite Element Modeling for Three-Dimensional Motion Reconstruction and Analysis. Computational Imaging and Vision, 2001, , 37-58.	0.6	6
144	The Future of Cardiac Magnetic Resonance Clinical Trials. JACC: Cardiovascular Imaging, 2021, , .	5.3	6

ALISTAIR A YOUNG

#	Article	IF	CITATIONS
145	Relative identifiability of anisotropic properties from magnetic resonance elastography. NMR in Biomedicine, 2018, 31, e3848.	2.8	5
146	Microstructural Remodelling and Mechanics of Hypertensive Heart Disease. Lecture Notes in Computer Science, 2015, , 382-389.	1.3	5
147	Determining Anisotropic Myocardial Stiffness from Magnetic Resonance Elastography: A Simulation Study. Lecture Notes in Computer Science, 2015, , 346-354.	1.3	4
148	Automated Personalised Human Left Ventricular FE Models to Investigate Heart Failure Mechanics. Lecture Notes in Computer Science, 2013, , 307-316.	1.3	4
149	Continuous Spatio-temporal Atlases of the Asymptomatic and Infarcted Hearts. Lecture Notes in Computer Science, 2014, , 143-151.	1.3	4
150	Regional Heterogeneity in 3D Myocardial Shortening in Hypertensive Left Ventricular Hypertrophy: A Cardiovascular CMR Tagging Substudy to the Life Study. Journal of Biomedical Science and Engineering, 2015, 08, 213-225.	0.4	4
151	The cardiac atlas project: rationale, design and preliminary results. Journal of Cardiovascular Magnetic Resonance, 2011, 13, .	3.3	3
152	Creating shape templates for patient specific biventricular modeling in congenital heart disease. , 2015, 2015, 679-82.		3
153	Quantifying passive myocardial stiffness and wall stress in heart failure patients using personalized ventricular mechanics. Journal of Cardiovascular Magnetic Resonance, 2016, 18, 017.	3.3	3
154	Left ventricular function and regional strain with subtlyâ€tagged steadyâ€state free precession feature tracking. Journal of Magnetic Resonance Imaging, 2018, 47, 787-797.	3.4	3
155	The Cardiac Atlas Project: Development of a Framework Integrating Cardiac Images and Models. Lecture Notes in Computer Science, 2010, , 54-64.	1.3	3
156	Quality-Aware Cine Cardiac MRI Reconstruction andÂAnalysis fromÂUndersampled K-Space Data. Lecture Notes in Computer Science, 2022, , 12-20.	1.3	3
157	CardiSort: a convolutional neural network for cross vendor automated sorting of cardiac MR images. European Radiology, 2022, 32, 5907-5920.	4.5	3
158	Localization and Atlas-Based Segmentation of the Heart from Cardiac MR Images: Validation with a Large Clinical Trial. , 2008, , .		2
159	Interactive biventricular modeling tools for clinical cardiac image analysis. Journal of Cardiovascular Magnetic Resonance, 2010, 12, .	3.3	2
160	The VPH-Physiome Project: Standards, tools and databases for multi-scale physiological modelling. Modeling, Simulation and Applications, 2012, , 205-250.	1.3	2
161	Computational analysis of cardiac structure and function in congenital heart disease: Translating discoveries to clinical strategies. Journal of Computational Science, 2021, 52, 101211.	2.9	2
162	Field-Based Parameterisation of Cardiac Muscle Structure from Diffusion Tensors. Lecture Notes in Computer Science, 2015, , 146-154.	1.3	2

#	Article	IF	CITATIONS
163	Estimation of In Vivo Myocardial Fibre Strain Using an Architectural Atlas of the Human Heart. Lecture Notes in Computer Science, 2013, , 208-215.	1.3	2
164	Comparison of 2D Echocardiography and Cardiac Cine MRI in the Assessment of Regional Left Ventricular Wall Thickness. Lecture Notes in Computer Science, 2020, , 52-62.	1.3	2
165	311 Finite element modeling integration of cardiac MRI structure and function. Journal of Cardiovascular Magnetic Resonance, 2008, 10, .	3.3	1
166	Recovery of Myocardial Kinematic Function without the Time History of External Loads. Eurasip Journal on Advances in Signal Processing, 2009, 2010, .	1.7	1
167	Imaging biomarkers for cardiovascular diseases. , 2020, , 401-428.		1
168	Sensitivity of Myocardial Stiffness Estimates to Inter-observer Variability in LV Geometric Modelling. Lecture Notes in Computer Science, 2021, , 287-295.	1.3	1
169	The Cardiac Atlas Project: Towards a Map of the Heart. , 2010, , 113-129.		1
170	Intraventricular Dyssynchrony Assessment Using Regional Contraction from LV Motion Models. Lecture Notes in Computer Science, 2013, , 458-465.	1.3	1
171	Interactive Cardiac Image Analysis for Biventricular Function of the Human Heart. Lecture Notes in Computer Science, 2010, , 144-153.	1.3	1
172	Patient Metadata-Constrained Shape Models for Cardiac Image Segmentation. Lecture Notes in Computer Science, 2016, , 98-107.	1.3	1
173	End-Diastolic and End-Systolic LV Morphology in the Presence of Cardiovascular Risk Factors: A UK Biobank Study. Lecture Notes in Computer Science, 2019, , 304-312.	1.3	1
174	Assessment of Thrombotic Risk following Transcatheter Mitral Valve Replacement. , 2021, , .		1
175	Fast modelling of heart pathology with soft objects. International Congress Series, 2005, 1281, 28-32.	0.2	0
176	2067 Scan-rescan reproducibility of left ventricular mass with 3D Cardiac Image Modeling (CIM). Journal of Cardiovascular Magnetic Resonance, 2008, 10, .	3.3	0
177	Accuracy of compressed sensing for left ventricular mass and volumes. Journal of Cardiovascular Magnetic Resonance, 2014, 16, P381.	3.3	0
178	Association of reduced right ventricular global and regional wall motion with abnormal right heart hemodynamics. Journal of Cardiovascular Magnetic Resonance, 2015, 17, P317.	3.3	0
179	Myocardial contractility and afterload in aortic stenosis. Journal of Cardiovascular Magnetic Resonance, 2015, 17, P371.	3.3	0
180	Regional Heterogeneity of LV Wall Thickness. JACC: Cardiovascular Imaging, 2015, 8, 1270-1271.	5.3	0

#	Article	IF	CITATIONS
181	Improving assessment of congenital heart disease through rapid patient specific modeling. , 2016, 2016, 1228-1231.		0
182	Parameterisation of Multi-directional Diffusion Weighted Magnetic Resonance Images of the Heart. Lecture Notes in Computer Science, 2016, , 60-68.	1.3	0
183	The Role of MRI in Preclinical and Clinical Functional Quantification and Modelling. , 2018, , 3-21.		0
184	The Cardiac Atlas Project: Rationale, Design and Procedures. Lecture Notes in Computer Science, 2010, , 36-45.	1.3	0
185	Investigating Heart Failure Using Ventricular Imaging and Modelling. Lecture Notes in Computer Science, 2010, , 164-173.	1.3	0
186	Maximum Likelihood Correction of Shape Bias Arising from Imaging Protocol: Application to Cardiac MRI. Lecture Notes in Computer Science, 2012, , 214-223.	1.3	0
187	Abstract 10282: Biventricular Shape Markers in Repaired Tetralogy of Fallot Associate with Pulmonary Valve Replacement Better Than Standard Clinical Indices. Circulation, 2021, 144, .	1.6	0